Available online at www.sciencedirect.com
ScienceDirect
Journal of Power Sources 180 (2008) 393–401
JOURNAL OF POWER SOURCES
www.elsevier.com/locate/jpowsour

Stress and plastic deformation of MEA in fuel cells Stresses generated during cell assembly

Daniil Bograchev [a], Mikael Gueguen [b], Jean-Claude Grandidier [b], Serguei Martemianov [c,*]

[a] *Frumkin Institute of Physical Chemistry and Elecrtrochemistry RAN, Leninski prospekt 31, Moscow 117071, Russia*
[b] *Laboratoire de Physique et Mécanique des Matériaux, LMPM UMR CNRS 6617, ENSMA, Téléport 2, 1 av. Clément Ader, BP 40109 86962 Futuroscope Cédex, France*
[c] *Laboratoire d'Etudes Thermiques, LET UMR CNRS 6608, ESIP-University of Poitiers, 40 av. du Recteur Pineau, 86022 Poitiers, France*

Received 5 December 2007; received in revised form 23 January 2008; accepted 3 February 2008
Available online 26 February 2008

Abstract

A linear elastic–plastic 2D model of fuel cell with hardening is developed for analysis of mechanical stresses in MEA arising in cell assembly procedure. The model includes the main components of real fuel cell (membrane, gas diffusion layers, graphite plates, and seal joints) and clamping elements (steel plates, bolts, nuts). The stress and plastic deformation in MEA are simulated with ABAQUS code taking into account the realistic clamping conditions. The stress distributions are obtained on the local and the global scales. The first one corresponds to the single tooth/channel structure. The global scale deals with features of the entire cell (the seal joint and the bolts). Experimental measurements of the residual membrane deformations have been provided at different bolts torques. The experimental data are in a good agreement with numerical predictions concerning the beginning of the plastic deformation.

Keywords: Fuel cell design; Proton exchange membrane (PEM); Nafion; Mechanical response; ABAQUS

1. Introduction

Proton exchange membrane fuel cell (PEMFC) is a possible substitute of combustion engine owing to its high efficiency and low level of pollutions. The PEMFC's operating characteristics, specifically durability, necessitate significant improvements [1]. The required lifetime of PEMFC exceeds 5000 h for automotive applications [2]. The PEMFC lifetime limitations can be caused by different factors. One of the reasons concerns with the loss of the conductivity properties of proton exchange membrane or degradation of catalyst layers [3]. Another reason deals with the thermo-mechanical deformation of membrane electrode assembly (MEA) which is the heart of PEMFC. Today Nafion® (Nafion® is registered trademark of sulfonated tetrafluorethylene copolymer by DuPont) is used usually as a material for membrane in fabrication of MEA. This polymer provides the protons transport from anode catalyst layer to cathode one and has unique thermal and mechanical stability. The membrane operates in chemical hostile environment with changes in temperature and humidity and under mechanical stresses. Today it is accepted that lifetime limitations of MEA are caused by chemical and thermo-mechanical factors. The general chemical factors are the decrease of electrochemical activity of catalytic layers and inter diffusion of platinum into membrane during fuel cell running.

Mechanical stresses which also limit durability of MEA have two origins. The first is the technology of fuel cell and stack assembly (bolt assembling). The function of the bolts deals with the necessity to assure the tightness and the electrical conductivity of contact elements. The contact pressure is one of the parameters which determine the performance of fuel cells [4,5]. Additional mechanical stresses arise during fuel cell running, because PEMFC consists of the materials with different thermal expansion and swelling coefficients. The temperature and the concentration gradients, which are associated with the gradients of material properties, generate mechanical stresses within fuel cell. In order to improve the durability of fuel cells, it is necessary to understand the phenomena which govern the arising

* Corresponding author. Tel.: +33 5 49 45 39 04.
E-mail address: serguei.martemianov@univ-poitiers.fr (S. Martemianov).

0378-7753/$ – see front matter © 2008 Elsevier B.V. All rights reserved.
doi:10.1016/j.jpowsour.2008.02.048

of pinholes and delamination between membrane and gas diffusion layer [6]. It is difficult to separate the mechanical, the thermal and the chemical effects in this problem. Besides, specific mechanical properties of Nafion®, as well as complexity and coupling of physical phenomena, compose a real scientific challenge to understand stresses and mechanical deformation arising in fuel cell during running.

The goal of several papers was an improvement of knowledge about mechanical stresses and plastic deformation within fuel cell. Regarding the physico-mechanical properties of Nafion®, it is possible to find sufficient information for predictive numerical simulations [7–10]. The problem of mechanical behavior of PEMFC has been studied in the review [11], where unavoidable difficulties of the multi-physical coupling have been considered. The possibility of mechanical failures of the membrane in fuel cell was discussed in [12]. Many works concern the mechanical behavior of the membrane [10–19]. Three recent works should be marked especially [17–19]. The membrane behavior under static hydro-thermal loading was investigated in [17]; the second work [18] was devoted to the mechanical stress evolution during the duty cycle (increasing/decreasing of the temperature and humidity). In the third one [19] the mechanical stress evolution was studied under humidity cycles at a constant working temperature (85 °C). The perfect plastic–elastic model of the membrane was assumed in [17,18] and the isotropic hardening model was used in [19]. The two modes of the fuel cell assembly were investigated in these works, namely *fixed force mode* corresponding to a case of fixed external stress, and *fixed displacement* mode corresponding to a case of initial compression and then a fixed displacement. The mechanical parameters of the membrane considering the temperature and humidity dependence are based on the work [10] data.

In the papers [17–19] the numerical simulations have been performed for the single tooth/channel configurations using 2D schematization. Thus, the obtained results reflect the local effects on the scale of only one channel. The gradients on the scale of entire fuel cell, in particular, the temperature and the mass fraction variation with respect to the distance from the entrance are not taken into account. So, the results cannot be used for the prediction of the edging effects near the seal joints. Moreover, the classical boundary conditions (displacement or force) do not reflect reality of the fuel cell assembling. Indeed, the bolts act as flexible elements which impose the different stress depending on their elongation and their stiffness.

The aim of the present paper is to fill up some gaps of the previous works [17–19]. This paper treats the numerical calculations of mechanical stresses arising in a single fuel cell during the assembling (cold model). The physical model of fuel cell, the numerical procedure and all parameters necessary for mechanical stresses calculation are presented with respect to the previous works. The calculations have been provided for a fuel cell geometry which is similar to the one used in the papers [17–19]. Nevertheless, a single tooth/channel configuration of the works [17–19] has been generalized in order to obtain the mechanical stresses in the entire fuel cell. More precisely, all the channels and the joints are taken into account in this model. Thus, the proposed configuration allows understanding of the border effects in the fuel cell. The stresses arising during cell assembling are discussed on the scale of one channel and on the scale of the entire cell.

2. Model definition

2.1. Geometry

The fuel cell has a complicated three-dimensional structure Fig. 1a and b; nevertheless, in this article a two-dimensional approach is used. Contrary to the previously proposed mod-

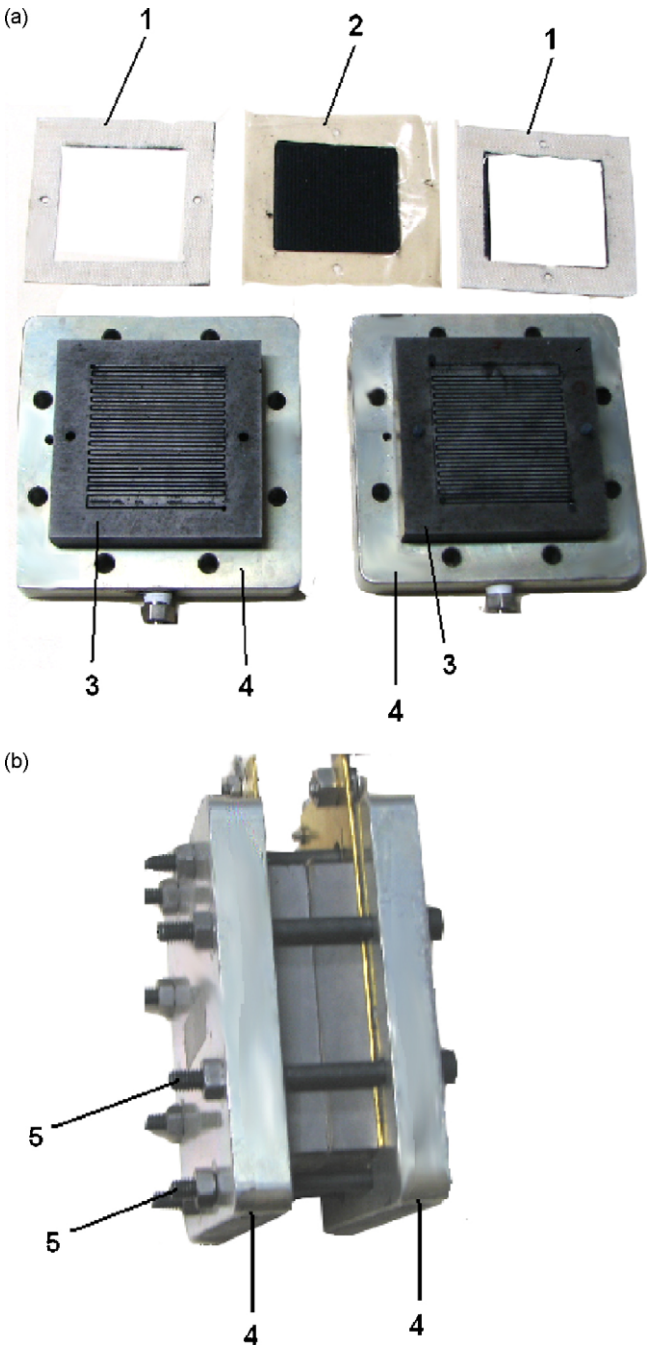

Fig. 1. (a) Fuel cell components and (b) fuel cell after assembly. (1) Seal joints, (2) MEA, (3) graphite plates, (4) steel plates and (5) bolts.

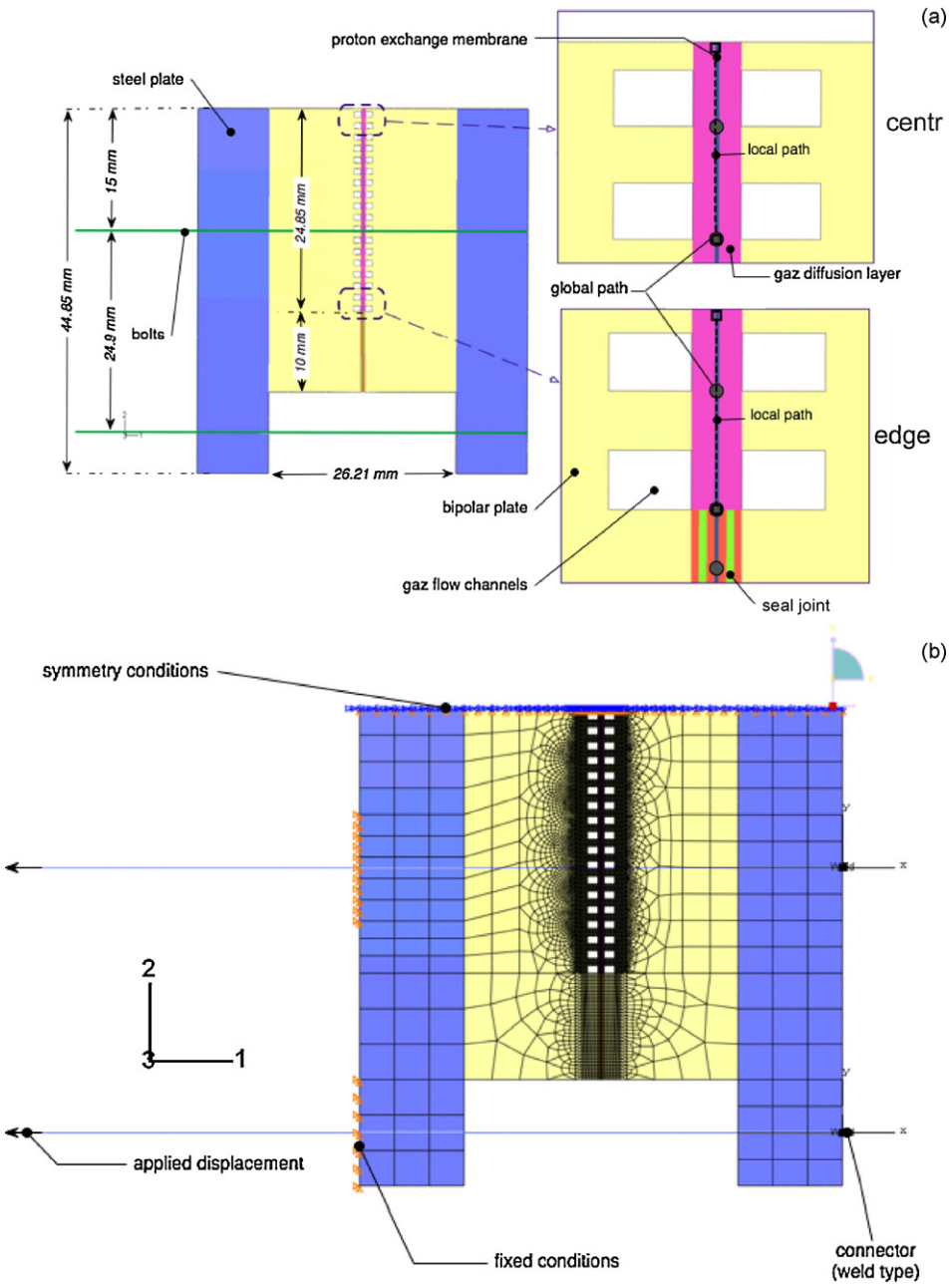

Fig. 2. (a) Schema of fuel cell model. (b) Mesh and boundary conditions.

els [17–19], the entire cross-section of a single fuel cell is considered in this study (see Fig. 2a). The present model consists of eight main parts: two steel plates, two graphite plates, two gas diffusion layers (GDL), a proton exchange membrane and a seal joint. In addition, there are two fastening elements (bolts) allowing a realistic simulation of applied loading. The catalytic layers are thinner than the membrane by one order of magnitude, thus it is possible to neglect their influence on mechanical phenomena, i.e. the catalytic layers are integrated into the gas diffusion layers. This assumption also was used in [17–19].

A symmetry condition is used in order to reduce the size of the problem, i.e. there is the axe of symmetry for all physical quantities. The schematic diagram of a half-cell is shown in Fig. 2a. Some sizes are defined in this figure, other parameters are the following: the thickness of the membrane (0.05 mm), the thickness of the steel plates (10 mm), the thickness of the GDE (0.28 mm), the length of the bolt (80 mm), the diameter f the bolt (5 mm) and the thickness of the seal joint (0.3 mm), the width of the tooth (0.7 mm) and the width of the channel (0.7 mm), the depth of channel (1 mm). The dimension which is perpendicular to a plane of cross-section (2D model) equals 100 mm. The numerical model has a periodic pattern with the opposite channels. A perfect assembling of different elements is supposed, the sliding is not taken into account and it is accepted that the stresses are transmitted completely on the interfaces.

This important hypothesis leads to an overestimation of stresses in the plane of the membrane.

2.2. Mesh

Commercial finite elements numerical code ABAQUS® v6.6 [20] has been used for numerical simulation of the fuel cell behavior, the local mesh is presented in Fig. 2b. The mesh includes 13,267 elements and 41,143 nodes. Coupled temperature-displacement elements with biquadratic interpolation for displacement and bilinear interpolation for temperature (CPEG8T and CPEG6MT) have been used. Generalized plane strain elements have been chosen in order to take into account more accurately the perpendicular stress in the bidimensional model. In order to allow the precise calculations in the proximity of two channels, the mesh has been refined in this zone (Fig. 2b). A particular attention has been put on the membrane and on a seal joint, two zones, which are the most sensitive to a fracture of fuel cells.

2.3. Mechanical properties

Mainly, the present model follows the one described in the works [17–19]. The mechanical properties of materials have been taken from [18,20,21]. The steel, the carbon paper and the graphite plate are assumed to have linear elastic behavior.

Seal joint has been made of Taconic®, which is composed by three layers of identical thickness: woven fiberglass coated with PTFE (polytetrafluoroethylene). Three layers of standard elements are used for modeling of seal joint, each layer is assumed to have elastic mechanical properties of fiberglass and PTFE.

Classical elasto-plastic model with isotropic hardening is accepted for Nafion® membrane. The corresponding data are given in Tables 1 and 2. It is important to note the restrictive character of the elasto-plastic model with respect to stress. More precisely, the membrane has actually viscoelastic behavior. As a consequence, the present model ignores the effect of relaxation of stress, the phenomenon which is intensified with the increase of the temperature. That is why obtained results give the overestimated values of stress.

In the elasto-plastic model, the total strain tensor components ε_{ij} are the sum of the elastic strain tensor components $\varepsilon_{ij}^{\mathrm{EL}}$ and the plastic strain tensor components $\varepsilon_{ij}^{\mathrm{PL}}$:

$$\varepsilon_{ij} = \varepsilon_{ij}^{\mathrm{EL}} + \varepsilon_{ij}^{\mathrm{PL}} \tag{1}$$

These strains are assumed to be small; this hypothesis is not very restrictive as the materials are confined within the assemblage. The material behaviors are assumed to be isotropic, and in the elastic region the Hooke's law is accepted. The constitutive law can be written as follows:

$$\sigma_{ij} = \frac{E}{(1+\nu)(1-2\nu)}(\nu\varepsilon_{ij}^{\mathrm{EL}} + \sum_k (1-2\nu)\varepsilon_{kk}^{\mathrm{EL}}\delta_{ij}) \tag{2}$$

where σ_{ij} are the stress tensor components, ν is the Poisson's ratio, E is the Young's modulus, ε_{ij} is the elastic strain tensor components, δ_{ij} is the Kroneker δ-symbol.

Table 1
Properties

Property	Value	Source
Nafion membrane		
Density, ρ (kg m^{-3})	2000	[18]
Young's modulus, E (MPa)	190 (300 K, 35% humidity)	[18]
Poisson's ratio (ν)	0.25	[18]
Yield strength, σ_0 (MPa)	See Table 2	[18]
Graphite plate		
Density, ρ (kg m^{-3})	1800	[18]
Young's modulus, E (GPa)	10	[18]
Poisson's ratio (ν)	0.25	[18]
GDE (carbon paper)		
Density, ρ (kg m^{-3})	400	[18]
Young's modulus, E (GPa)	10	[18]
Poisson's ratio (ν)	0.25	[18]
Seal joint (40% woven fiberglass E–60% PTFE)		
Density, ρ (kg m^{-3})	PTFE 2200; fiberglass E 2540	[21]
Young's modulus, E (GPa)	PTFE 0.8; fiberglass E 72	[21]
Poisson's ratio (ν)	PTFE 0.46; fiberglass E 0.22	[21]
Steel		
Density, ρ (kg m^{-3})	7800	[20]
Young's modulus, E (GPa)	209	[20]
Poisson's ratio (ν)	0.25	[20]

The plasticity behavior is described by Prandtl-Reuss theory. The Von Mises yield function is written as follows:

$$f(\sigma_{ij}) = \sqrt{\frac{3}{2}S_{ij}S_{ij}} - \sigma_0 \tag{3}$$

and the Von Mises yield criterion is reduced to

$$f(\sigma_{ij}) = 0 \tag{4}$$

where $S_{ij} = \sigma_{ij} - (1/3)\sigma_{\mathrm{kk}}$, δ_{ij} is the deviatoric stress tensor components. The plasticity evolves when $f(\sigma_{ij}) > 0$. Plasticity evolutions are described by isotropic hardening curves of Nafion® which are taken from work [10]. According to the Prandtl-Reuss theory, the plastic increment tensor is proportional to the derivative of the yield function f given by Eq. (3):

$$\mathrm{d}\varepsilon_{ij} = -\frac{\partial f}{\partial \sigma_{ij}}\mathrm{d}\lambda \tag{5}$$

where $\mathrm{d}\lambda$ is the plastic multiplier calculated by the consistent relation ($\mathrm{d}f = 0$) during the hardening. The plastic multiplier corresponds to the increment of equivalent plastic strain.

Table 2
Set of the hardening curve of Nafion [10]

Yield strength (MPa)	Equivalent plastic strain
6.60	0
6.60	0.167
15.4	2.09

2.4. Mechanical loading (method of assembly)

In recent works [17–19], the mechanical loading of fuel cell has been considered using two schematizations: relative displacement of two plates and application of a given force. Both schematizations do not reflect reality and are used for approximation of the stresses in the fuel cell elements. Contrary to this traditional way, a more realistic approach is used in the present study which takes into account the presence of the bolts in the assembly. The bolts are modelled by the beams with circular section (type B21 in ABAQUS®), which are attached to one of the plates using the connector join (type CONN2D2 in ABAQUS®). The connection between the 2D mesh and the beam is realized by means of the total elimination of the degree of freedom in order to assume the perfect transmission of the forces and the moments from the head of the bolts to the plate. On the opposite plate, in the place where the nuts press the surface, the displacement in the normal direction is forbidden (see Fig. 2b). The loading is applied by a displacement of the second edge of the beam; this displacement reflects the loading arising during application of a moment of forces to the bolt. The displacement is imposed gradually and the contact pressure between the elements of the fuel cell is governed by the stiffness of the bolts. The size and the elasticity modulus of the bolts in the model have been chosen with respect to the ones used in the real assembling procedure.

In the real 3D configuration the bolts are disposed around the entire cell with aim to apply homogeneous contact pressure between Nafion® membrane, GDL and graphite plates. In order to make the 2D modeling more realistic, two loading beams are used in this study. Actually, this choice influences the local loading distribution. However, we have verified afterwards that 2D model allows rather good simulating of homogeneous pressure distribution for the case of two parallelepiped plates joined by two loading beams.

The reduction from the real 3D configuration to 2D model requires estimation of the normal stress provided by bolts in numerical schema for a given bolt torque (real experimental value). It can be done by adjusting of the displacement applied to the edges of the both beams in numerical calculations to the one generated in the real fuel cell. In other words, a normal stress between graphite plate and steel plate in numerical calculations should be close to the mean pressure arising in a real fuel cell. This pressure allows establishing of a simple relation between displacement of beams in numerical model and bolts torque applied during cell assembly procedure.

It has been calculated that the applied displacement $d_{IMP} = 0.038$ mm allows obtaining of the average value 1 MPa for the normal stress on the interface between graphite and steel plates. This value of loading has been accepted in [17–19] and is used as the reference in this work. In the present study gradually increasing load is used which is applied at the room temperature 27 °C and at moisture content of the Nafion® membrane being equal to 35%. In the real 3D configuration the bolts are disposed around the entire cell with the aim to apply homogeneous contact pressure between Nafion® membrane, GDL and graphite plates. In order to make the 2D modeling more realistic, two loading beams are used in this study. Naturally, this choice influences the local loading distribution, but we have verified afterwards that 2D model allows rather good simulating of homogeneous pressure distribution for the case of two parallelepiped plate joined by two loading beams. The distribution of the normal stresses is presented in Fig. 3. Note that the normal stresses are not constant, with the important values near the edge of the cell and relatively homogeneous central zone. The values of the normal stress in the edge of the cell are obtained under the assumption that assembly is perfect (sliding between different elements is not taken into account). In the central zone, according to the global path, the mean stress value equals 1.0 MPa for the displacement $d_{IMP} = 0.038$ mm. The corresponding pressing force applied to the beams equals $F = 1865$ N.

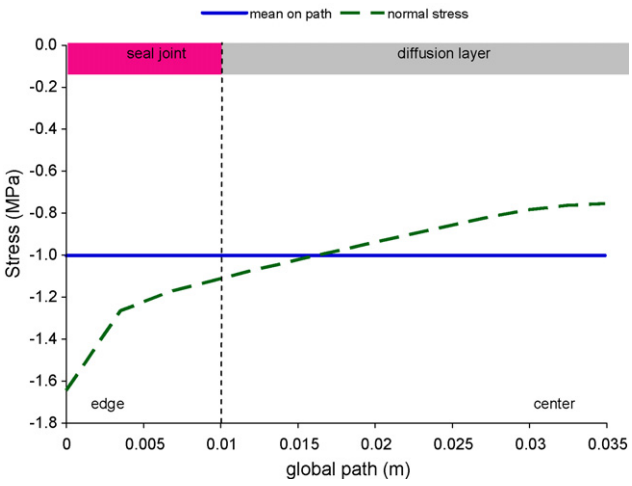

Fig. 3. Normal stress distribution.

Using classical relation, it is possible to calculate the tightening torque C as a function of F the tension applied to the screw, μ the friction of the thread and the bolt, α inclination of the thread:

$$C = \frac{F(\mu D_{ma} + \mu D_{mf} + D_{mf}\tan(\alpha))}{2} \quad (6)$$

where D_{ma} is the average diameter of the contact zone between the head and the steel plate, D_{mf} is the diameter of the thread and α is the angle of the thread pitch. Taking into account the characteristics of standard screw used in the laboratory (type M6 80) and accepting that the friction coefficient μ is approximately equal to 0.2 (dry assembling), the experimental tightening torque C is estimated as 2.32 Nm for the contact pressure of about 1 MPa.

3. Numerical results and discussion

In this paragraph the distribution of the stresses in the membrane is evaluated on two scales. The local scale deals with a single tooth/channel configuration; the global one allows obtaining of the mechanical stresses in the entire fuel cell. The local analysis has been performed in the cell center region (near the axis of symmetry) and in the cell edge region (see Fig. 2a, the small dots in the zoomed pictures). Both regions include two channels to emphasize a periodic character of the local fields.

The stresses distribution on the scale of the entire cell is presented with a particular global path. This path goes through the membrane center points which are situated in front of the lowest corners of the channels (see Fig. 2a, the big dots in the zoomed pictures). The path goes also under the joint which gathers around the membrane in order to visualize the concentration of the stresses in this transitional zone. The normal direction 1 is perpendicular to the MEA and the transverse directions 2 and 3 are situated in the plane of the MEA; the direction 3 is perpendicular to the plane of the model (see Fig. 2b).

3.1. Global distribution

The results of calculations of the stress field on the entire cell scale are presented in Fig. 4. The stress distribution is inhomogeneous in Nafion® under the interface between seal joint and diffusion layer. This strong discontinuity of the stresses under this interface affects all the components of the stress tensor. In the membrane the most important component of the stress is the normal one. It can be denoted as σ_{11} (in the direction 1), which is negative along the membrane surface; this corresponds to the

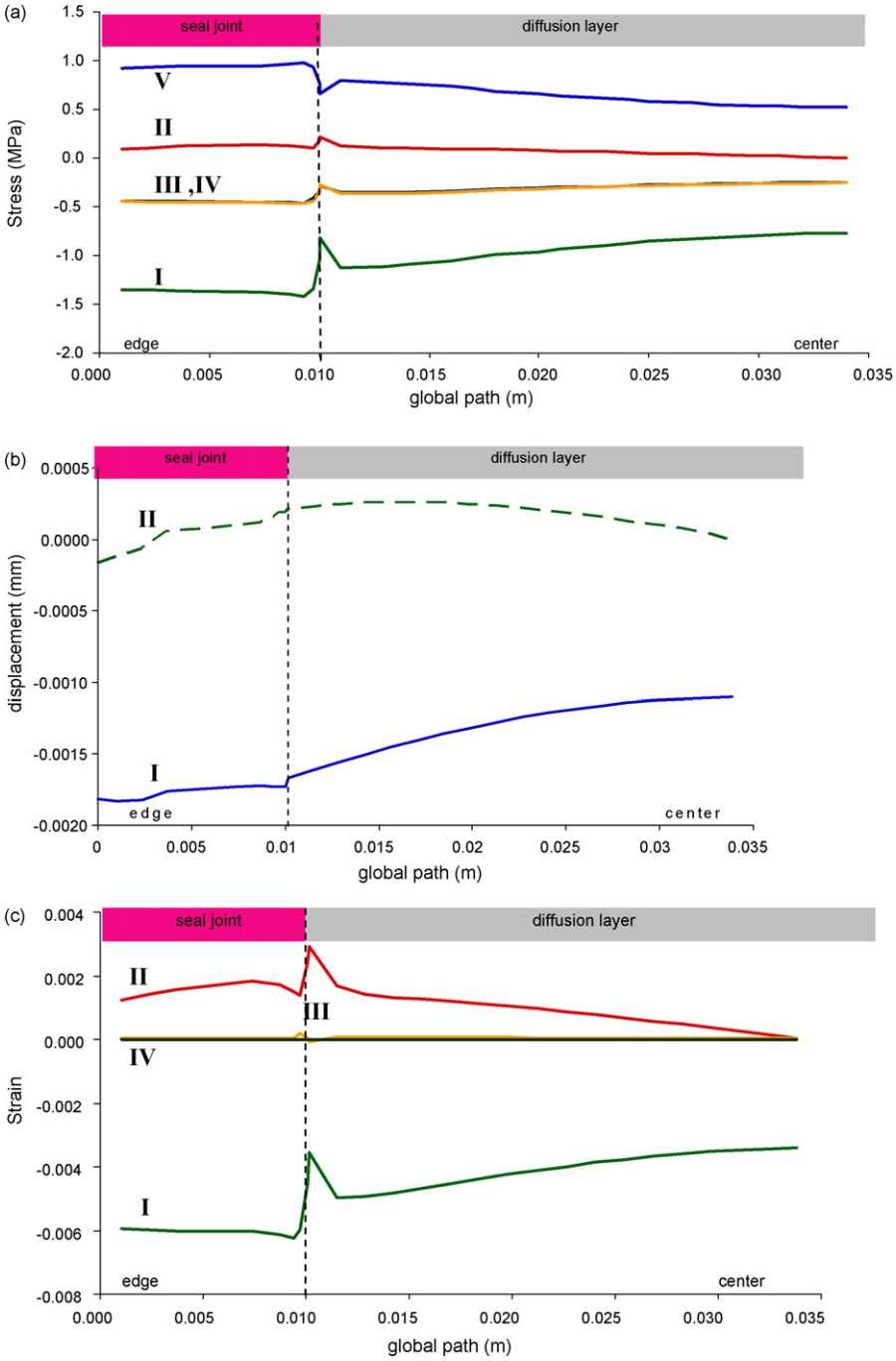

Fig. 4. Distribution along membrane: stresses (a); displacements (b); strains (c). (a) **I**, normal stress; **II**, shear stress; **III**, tangential stress out of plane; **IV**, tangential stress; **V**, Mises stress. (b) **I**, normal displacement; **II**, tangential displacement. (c) **I**, normal strain; **II**, shear strain; **III**, tangential strain out of plane; **IV**, tangential strain.

state of the compression which is necessary for the good performance of the cell. So, in this configuration the joint assumes its function. The transversal stresses (noted σ_{22} and σ_{33}) are also negative and significantly smaller than the normal stress. The both components σ_{22} and σ_{33} are equal; this is an interesting result which justifies the choice of the generalized plane deformation elements in the computational procedure. These elements have allowed obtaining of a solution which is identical in the transversal directions 2 and 3. It is a realistic result for the case of square graphite plates. The transversal stresses are negative because the model ignores sliding between the elements of assembly. Naturally, the transversal stresses can decrease when the sliding occurs. It has been noted that the ratio between the normal and the tangential stresses is about 3. The shear stresses are by one order of the magnitude smaller, but a peak can be observed under the joint/diffusion interface. Near the cell centre the stresses decrease slightly with respect to the values obtained near the joints. The average value of the Mises stresses is about 0.72 MPa in the central part of the cell. Under the seal joint, the compressive load in the membrane is higher than 1 MPa (mean value imposed by bolts). However, under the diffusion layer the compressive stress is lower than mean value.

The displacement of the mean plane of the membrane (see Fig. 4b) shows that the structure is bended due to the bolts load. The shear and normal strain components have a distribution similar to shear and normal stress (see Fig. 4c). It should be noted that the transversal components ε_{22} and ε_{33} are very small due to non-sliding conditions. The shear strain and normal strain have the same level. Under the joint/diffusion layer interface the maximal strain reaches −0.06% for normal strain and 0.03% for shear strain. The shear strains are relatively important in comparison with the compression state.

The strong discontinuity observed near the joint confirms the experimental fact, that the junction is the zone sensible to failure. Thus, non-uniformity of the stresses during assembly (cold model) is caused by the structural features and non-uniform displacement (see Fig. 4b) generated by assembling elements. Pressure is higher in the cell edge than in the cell centre due to bending of the steel plates under the action of loading bolts. The difference between stiffness of seal joint (composite PTFE/woven fiberglass) and stiffness of gas diffusion layer (carbon paper) (see Table 1) is the principal factor responsible for the singularity of the compressive stress at joint/diffusion layer interface. It is noteworthy that in our model the plastic strain is not reached when the applied pressure is equal to 1 MPa as well as in the articles [17–19] under the identical conditions.

3.2. Local distribution

The local fields of the stress in membrane have periodic evolution in phase with the periodicity of the channels. This result is obtained for all components of the stress tensor. The maximum amplitudes of stress oscillations are localized next to edge of the fuel cell and they are in order of 1 MPa for the normal stress σ_{11}, 0.15 MPa for shear stress σ_{12}, and 0.30 MPa for tangential stresses σ_{22} and σ_{33}. Normal and tangential stress amplitudes are almost constant on local path, contrary to shear stress. The

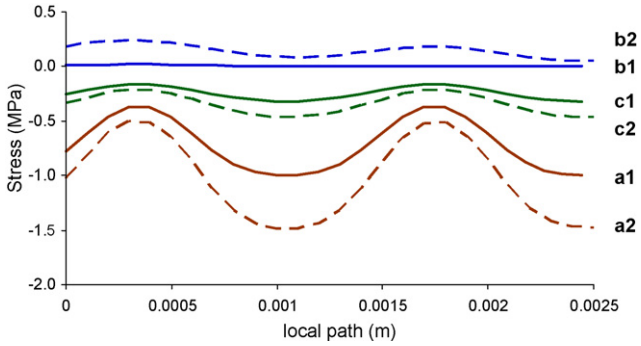

Fig. 5. Normal (a), shear (b) and tangential (c) stresses distribution center (1) and at edge (2) region of membrane.

difference of local values at a given position for each channel allows to quantify the global evolution on the channel scale (values at $x = 0$ m and $x = 0.0015$ m on Fig. 5). These variations are small in comparison to local oscillation of stress field. From the local point of view, the stress state is strongly inhomogeneous. However, it should be marked that the shear stresses are relatively important on the border of the cell and are higher than center's ones. The level of normal stress is also more important than the tangential and shear stress at the local scale, this point confirms the results observed at a global scale.

In summary, important variations of stresses (local or global) generated during the assembling procedure can be a source of the limitation of the mechanical reliability of the system.

3.3. Relation between plasticity and torque

The calculations have been performed in order to determining the torque which can cause the plastic effect in the membrane due to mechanical load. The obtained results correspond to 15.8 Nm (curve 680% in Fig. 6); this reflects the displacement of 0.258 mm imposed to the tightened screw. In this case the plasticity arises in the membrane under the seal joint (junction joint/diffusion plate), the level of the equivalent plastic strain is

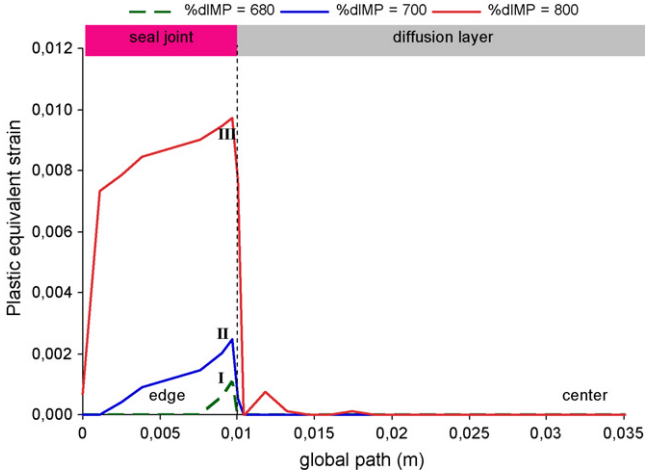

Fig. 6. Equivalent plastic strain for different initial loading 680% (**I**); 700% (**II**); 800% (**III**); 100% corresponds to loading which generates normal stress of 1 MPa.

nearly equal to 0.001. The value of pressure in the graphite plate is about 7.3 MPa. The plastic zone expands under the seal joint and the level of equivalent plastic strain rises with the increase of compression (see Fig. 6) The curve 700% corresponds to the displacement of 0.266 mm with tightening torque which is equal to 16.3 Nm, and the curve 800% corresponds to a displacement of 30.4×10^{-2} mm with tightening torque which is equal to 18.6 Nm.

The influence of the torque on the fuel cell performance has been studied in [4,5]. The maximal performance in these studies has been obtained with the compression moment of about 9 Nm. The cell assembly in this work has been provided by the screw bolts of M6 80 type. Taking into account the number of the bolts and the surface of the MEA, it is possible to estimate the pressure in the graphite plate: 4.1 MPa. These estimations show that the applied mechanical loading can be considerably larger than the one used in [17–19] for the numerical simulations in optimized experimental conditions. That is why the risk of the plastic effect and the membrane damage may be higher with respect to previous predictions [17–19]. In consequence, it is necessary to take carefully into account the initial mechanical loading of the cell.

4. Experimental verification of the model

The main aim of this paper is the development of the complex model which predicts mechanical behavior of MEA during assembly. This model is based on some assumptions; the most important of them concerns the dimensional reduction from 3D to 2D and mechanical behavior of Nafion® in the thickness direction. Naturally, the question of experimental verification of the model is very significant.

In this paragraph the results of the experiment related to measurements of residual deformation arising in MEA after cell assembling are presented. The residual deformations have been identified by recording of the membrane thickness before and after cell assembling without fuel cell running. For the thickness measurements TESA® Microster IP54 has been used; the MEA has been fabricated by hot pressing using Nafion 112 membrane and Taron® TPG-H as GDL.

The cell has been assembled with Taconic® woven fibreglass seal joints. The FACOM® dynamometric key allowing measurements of applied torque has been used for bolts twisting. At first, the fuel cell has been clamped by the smallest bolts torque and then the bolts torque has been increased in discrete steps. At the every step the fuel cell has been disassembled and the membrane thickness at six selected points has been measured.

The location of the selected points for the thickness measurements on the surface of MEA is shown in Fig. 7. These points have been chosen under seal joint region where, according to numerical simulations, the deformations are the most significant and plasticity arises early. The initial thicknesses of the selected points are shown in Table 3. The results of residual deformation measurements at different bolt torques are presented in Fig. 8. There is a sharp turn in evolution of the residual deformation under the bolts torque magnitude which is approximately equal to $N^* \approx 16$ Nm. The sudden change of the membrane thickness

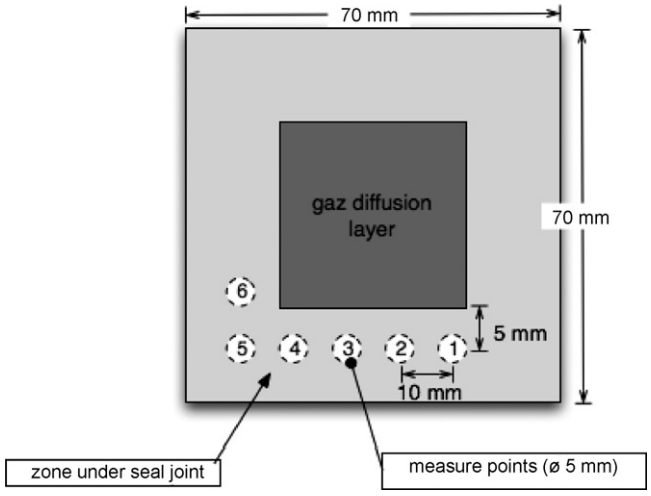

Fig. 7. Location of the selected points for the thickness measurements on the MEA surface.

Table 3
The initial membrane thickness in selected points

The point number	The membrane thickness, ±0.8 (μm)
1	58
2	58
3	58
4	58
5	57
6	57.7

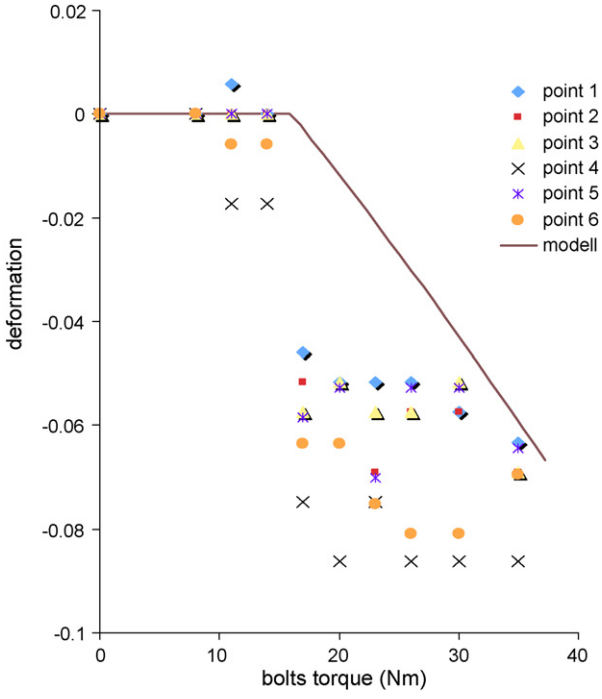

Fig. 8. Residual deformation of membrane at different bolt torques. Markers correspond to experimental results; the solid line presents result of numerical simulations.

can bee interpreted as a beginning of plastic deformation. For the comparison in Fig. 8 we also present the results of the numerical simulations. It can be noticed that numerical simulations are in a good agreement with experimental data concerning the beginning of the plasticity deformation.

From the other hand, there is a clear difference between numerical predictions and experimentally obtained deformations for the bolts torque in the range of $16\,\text{Nm} < N < 35\,\text{Nm}$. The numerical model predicts a linear evolution of the residual deformation with the increasing of bolts torque. The measurements show that deformation turns sharply at the critical value $N^* = 16\,\text{Nm}$ and becomes approximately constant for $N > N^*$. Under the bolts torque equal to $N \approx 35\,\text{Nm}$ the experimental and numerical values of residual deformations are approximately the same. The difference between the measurements and theoretical prediction is due to the hardening curve of Nafion®. Nevertheless, this difference is reasonably small. Provided experiments show that the developed model can predict correctly the main mechanical phenomena in MEA during assembly procedure.

5. Conclusion

In this article the mechanical stresses generated in the fuel cell during assembly have been studied numerically and, furthermore, developed model has been compared with experimental data.

The simulations have been provided using 2D finite elements model representing the entire fuel cell. Linear elastic model has been used for the cell components except the membrane which has elasto-plastic behavior with hardening. The realistic assembly procedure is simulated taking into account mechanical action of flexible bolts. The developed model allows understanding of the stress distributions on the local and the global scales. On the scale of single tooth/channel structure the stress distribution in the membrane is not uniform and the stresses have a periodic character. The stress evolutions along the membrane have been obtained on the scale of the entire cell as well. In particular, a zone with strong heterogeneous stresses in membrane under the junction seal joint/graphite plate has been observed and quantified. This heterogeneity is caused mainly by the structural features and by the difference between stiffness of seal joint and gas diffusion layer. At the applied mechanical load corresponding to 1 MPa, the membrane does not reach the plasticity. Calculations show that the membrane reaches plasticity under the torque which is equal 15.8 Nm. The plasticity arises primarily in the zone of the maximal stresses, i.e. under the junction seal joint/graphite plate.

The developed model has been compared with experimental data. In these experiments the residual deformations in the membrane have been determined by measuring the membrane thickness before and after assembly procedure at different bolts torques. These measurements have been provided in the thicknesses edge zone (under the seal joint). The experimental data show a sharp turn in evolution of the residual deformation under the bolts torque magnitude which is approximately equal to $N^* \approx 16\,\text{Nm}$. This fact can be interpreted as the beginning of plastic deformation. It can be noticed that experimental data agree well with numerical calculations with respect to the beginning of the plastic deformation.

Acknowledgment

The authors thank the Federation of laboratories P'PRIMME for financial support of this work.

References

[1] S.J. Chalk, J.F. Miller, Journal of Power Sources 159 (2006) 73–83.
[2] M.F. Mathias, et al., Electrochemical Society Interface 14 (2005) 24–35.
[3] G. Hinds, Performance and Durability of PEM Fuel Cells: A Review, Dr. M.G. Gee, Knowledge Leader, NPL Report DEPC-MPE 002, 2004.
[4] J.-J. Kadjo, J.-P. Garnier, J.-P. Maye, F. Relot, S. Martemianov, Russian Journal of Electrochemistry 42 (2006) 467–475.
[5] J.-J. Kadjo, P. Brault, A. Caillard, C. Coutanceau, J.-P. Garnier, S. Martemianov, Journal of Power Sources 172 (2007) 613–622.
[6] S. Kundu, M.W. Fowler, L.C. Simon, S. Grot, Journal of Power Sources 157 (2006) 650–656.
[7] T. Takamatsu, A. Eisenberg, Journal of Applied Polymer Science 24 (1979) 2221–2235.
[8] Uan-Zo-li JulieTammy, The Effects of Structure, Humidity and Aging on the Mechanical Properties of Polymeric Ionomers for Fuel Cell Applications, Virginia Tech, 2001.
[9] Y. Kawano, Yanqia Wang, R.A. Palmer, S.R. Aubuchon, Polimeros: Ciencia e Tecnolofia 12 (2002) 96–101.
[10] Y. Tang, et al., Materials Science and Engineering A 425 (2006) 297–304.
[11] V. Mehta, J.S. Cooper, Journal of Power Sources 114 (2003) 32–53.
[12] A.Z. Weber, J. Newman, AIChE Journal 50 (2004) 3215–3226.
[13] C.S. Gittleman, Y.-H. Lai, C. Lewis, D. Miller, Proceedings of the AIChE Annual Meeting, Cincinnati, OH, 2005.
[14] J. Xie, D.L. Wood III, K.L. More, P. Atanassov, R.L. Borup, Journal of the Electrochemical Society 152 (2005) A1011–A1020.
[15] V. Stanic, M. Hoberecht, Mechanism of pin-hole formation in membrane electrode assemblies for PEM fuel cells, in: Proceedings of the 4th International Symposium on Proton Conducting Membrane Fuel Cells, 2004, p. 1891.
[16] Y. Lai, M. Budinski, C.S. Gittleman, D.A. Dillard, Tear resistance of proton exchange membranes, in: Proceedings of the 3rd International Conference on Fuel Cell Science, Engineering and Technology, Ypsilanti, Michigan, May 23–25, 2005, pp. 153–159.
[17] Y. Tang, M.H. Santare, A.M. Karlsson, S. Cleghorn, W.B. Johnson, J. Fuel Cell Sci. Technol. 3 (2006) 119–124.
[18] A. Kusoglu, A.M. Karlsson, M.H. Santare, S. Cleghorn, W.B. Johnson, Journal of Power Sources 161 (2006) 987–996.
[19] A. Kusoglu, A.M. Karlsson, M.H. Santare, S. Cleghorn, B.J. William, Journal of Power Sources 170 (2007) 345–358.
[20] ABAQUS Analysis User's Manual, V6.6, HKS, 2006.
[21] Product information of Tonoga Inc., 2005.